Scientific report

on the project implementation in the period January 2012 – December 2014

"TiO_2/ZrO_2 thin films synthesized by PLD in low pressure N-, C- and/or O-containing gases: structural, optical and photocatalytic properties", O. Linnik, I. Petrik, N. Smirnova, V. Kandyba, O. Korduban, A. Eremenko, G. Socol, N. Stefan, C. Ristoscu, I. N. Mihailescu, C. Sutan, V. Malinovski, V. Djokic, Dj. Janakovic, Digest Journal of Nanomaterials and Biostructures, Vol. 7(3) (July–September 2012), 1343-1352 (**2012**)

Doped TiO_2/ZrO_2 films were obtained by Pulsed Laser Deposition (PLD) method under different synthesis conditions. The onset of absorption spectra was red shifted for the films obtained in N_2 containing gas mixtures, while a broad absorption in visible was observed in the case of films deposited in CH_4 atmosphere. The presence of O-Ti-N bonds revealed by XPS corresponded to the highest photocatalytic performance. XPS spectra of the samples obtained in N_2/CH_4 gas mixtures evidenced a more effective incorporation of nitrogen in the structure due to oxygen deficiency. Nevertheless, no atomic carbon presence in the TiO_2/ZrO_2 structures has been detected.

The photocatalytic activity of doped films was monitored in the process of the toxic Cr(VI) ions photoreduction to non-toxic Cr(III) ions in aqueous media by exposure to visible or UV light. The films were inert under visible light irradiation showing an activity similar to that of blank sample. Bare zirconium oxide film possessed much lower activity comparing to bare TiO_2 film under UV light. An improvement of the photocatalytic performance compared to TiO_2 film was observed under UV light exposure of TiO_2/ZrO_2 film containing double doping agent (TZ5). The highest reaction rate constant (Table I) was reached for the structure with the largest number of O-Ti-N bonds. We suggest that the O-Ti-N bonds (Eb = 395.8 eV) improve the electron-hole separation, while the interstitial N atoms (Eb = 400.0 eV) incorporated in semiconductor structure are inert as the electron/hole traps in photoreduction under UV and Vis - light irradiation.

Sample	*K, sec^{-1}*
TZ1	*$3,1*10^{-5}$*
TZ2	*$3*10^{-5}$*
TZ3	*$3,5*10^{-5}$*
TZ4	*$3,5*10^{-5}$*
TZ5	***$8,4*10^{-5}$***
TZ6	*$2,2*10^{-5}$*
TZ7	*$2,5*10^{-5}$*
TiO_2	*$7,0*10^{-5}$*
ZrO_2	*$2,2*10^{-5}$*

Table I. The reaction rate constant of studied samples for Cr^{6+} to Cr^{3+} photoreduction under full light irradiation

Thus, the TiO_2 band-gap narrowing is mandatory for extending the photocatalytic action to visible light. Nevertheless, other factors such as an effective trapping of photogenerated charge carriers, adsorption/desorption of reaction components and appropriate redox couples could crucially influence the recombination rate of an electron-hole pair.

„*Measuring Nanolayer Profiles of Various Materials by Evanescent Light Technique*", N. Mirchin, B. Apter, I. Lapsker, V. Fogel, U. Gorodetsky, S. A. Popescu, A. Peled, G. Popescu-Pelin, G. Dorcioman, L. Duta, A. Popescu, I. N. Mihailescu, Journal of Nanoscience and Nanotechnology, Vol. 12(3), pp. 2668–2671, **2012**

The evanescent light photon extraction efficiency of insulator, semiconductor and conductor amorphous nanolayers deposited on glass waveguides was evaluated from Differential Evanescent Light Intensity measurements. The Differential Evanescent Light Intensity (DELI) technique uses the evanescent field scattered by the deposited nanolayer, enabling nanometer thickness profiling due to the high inherent dark background contrast. The results show that the effective evanescent photon penetration depth increases from metal to semiconductor and then to insulating layers, establishing thus the effective photon-material interaction length for the various materials classes.

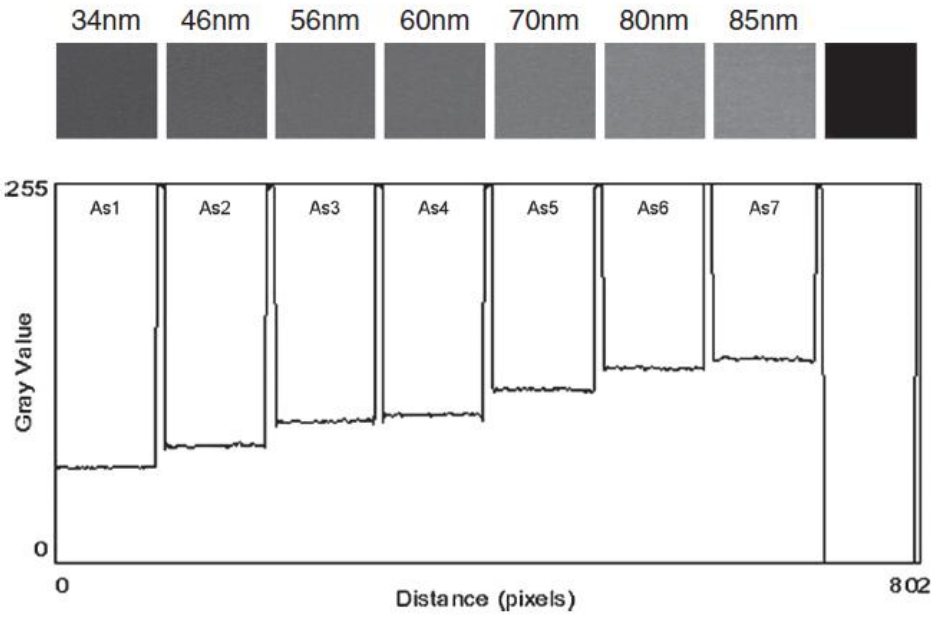

Fig. 1. Upper square figures are the DELI 2D images of the seven a-Au sampled area profiles of (842×842) μm^2 for discrete thicknesses in the range (34–85) nm. Beneath the 2D square zones images the 1D profile averaged over vertical y-coordinate across each of the 2D areas are shown. The black zone is for calibration purposes.

In our DELI technique the light power extracted from the waveguide depends on the thickness and number of deposited nanoparticles on the surface. Due to spatial varying adsorption properties for instance, the nanolayers may have various coverage properties. In the non-deposited areas, complete TIR occurs for the trapped light propagating in the waveguide and no light comes out, see black zone in Figure 1. The nanometer thick deposited areas extract the light from the evanescent waves approximately in proportion to their thickness up to an effective thickness of the photon–material interaction.

The DELI technique, based on capturing the evanescent field scattered by a nanolayer has the advantage over reflective or transmission microscopy that the propagating electromagnetic field in the waveguide does not interfere with the field extracted perpendicular to the substrate surface. It thus guaranties an excellent dark background contrast enabling direct depth *z*-direction optical microscopy nanometer thickness profiling. For insulator nanolayers the technique has a longer range of interaction with the

evanescent photons as compared to semiconductors and conductors. Accordingly, thicker films fall in the range suitable for DELI nanometer profiling, up to about 200 nm. There is no risk of nanomaterials damage because they are not exposed in DELI to the direct action of intense light or electron beams. The technique is much easier and economical for nanometer films profiling as compared to SEM and AFM and suited especially for large areas profiling needed in industrial applications.

"Nanoprofiles evaluation of ZnO thin films by an evanescent light method", N. Mirchin, A. Peled, L Duta, A. C. Popescu, G. Dorcioman and I. N. Mihailescu, Microscopy Research and Technique 76 (10) 992-996, **2013**

The extraction efficiency of evanescent light from ZnO nanolayers and their thickness profiles in the range of (1–105) nm was evaluated by a new microscopy technique, differential evanescent light intensity imaging method. It is based on capturing the evanescent light scattered by the layer of the material deposited on glass substrates. The analyzed ZnO films were obtained by pulsed laser deposition at 27 C and 100 C, using a nanosecond UV laser source.

In Fig. 2 are presented DELI Images of the ZnO structures along with their 1D profiles.

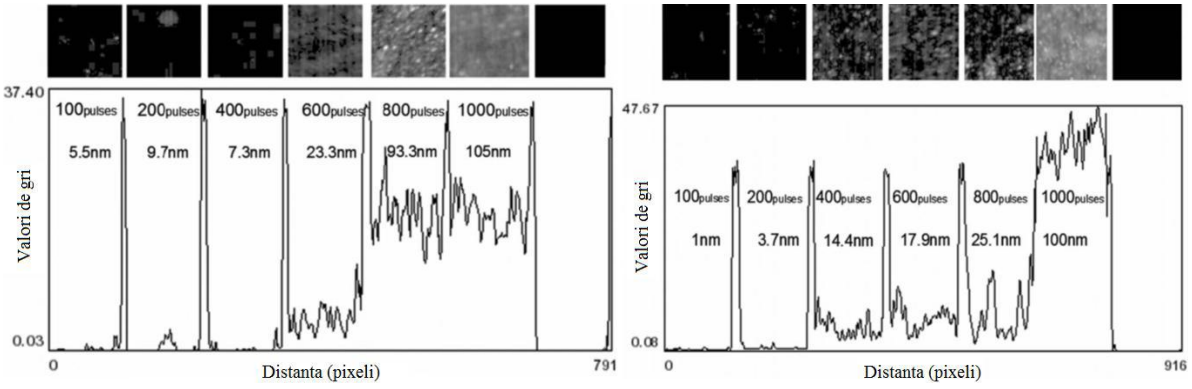

(a) (b)

Fig. 2. DELI 2D images of six ZnO films samples deposited at 27C (a) and 100 C (b) with 100–1000 laser pulses, with areas of (520x520) μm^2 and mean thicknesses in the range of (5.5–105) (a) and (1-100) (b) nm. Below the 2D square zone images, the x-direction 1D thickness profiles averaged over the y-coordinate across each of the 2D areas are shown. The black square at the right side is the undeposited zone image on the waveguide used for calibration.

We used the nanometer profile diagnostic method DELI to infer the photon extraction efficiency *γ* of ZnO nanolayers deposited by PLD at two different temperatures, of 27C and 100C. The values obtained of 0.01235 and 0.01146 nm^{-1} were close to results obtained for other insulators such as polyethylene, for which *γ* was about 0.0079 nm^{-1}. The DELI optical z-profiling method proved to be sensitive enough to observe film thickness variations in the range of (1–105) nm.

"*Enhancing the gas sensitivity of oxide thin films by surface structuring"*, G. Socol, F. Sima, E. Axente, C. Ristoscu, N. Stefan, M. Socol, C.R. Luculescu, I.N. Mihailescu, Poster presentation at symposium O: Synthesis, processing and characterization of nanoscale multi functional oxide films IV of the E-MRS 2013 Spring Meeting, Congress Center in Strasbourg (France) from May 27 to 31, **2013**.

Binary mixtures in different atomic ratios of metallic oxide thin films were deposited by PLD technique. The coatings were prepared by ablation of ZnO-SnO_2 targets in low oxygen pressure and elevated substrate temperatures. The oxide thin films were surface structured by laser irradiations using a KrF* excimer source or via plasma treatment. In the case of laser surface texturing experiments, a beam homogenizer was used in order to ensure a uniform energy distribution across the entire area. The most important laser irradiation parameters proved to be the laser fluence and number of pulses. XRD analyses evidenced that the coatings of oxide mixtures were polycrystalline (Fig. 3). Selected samples were subjected to gas sensing investigations on the base of a testing protocol.

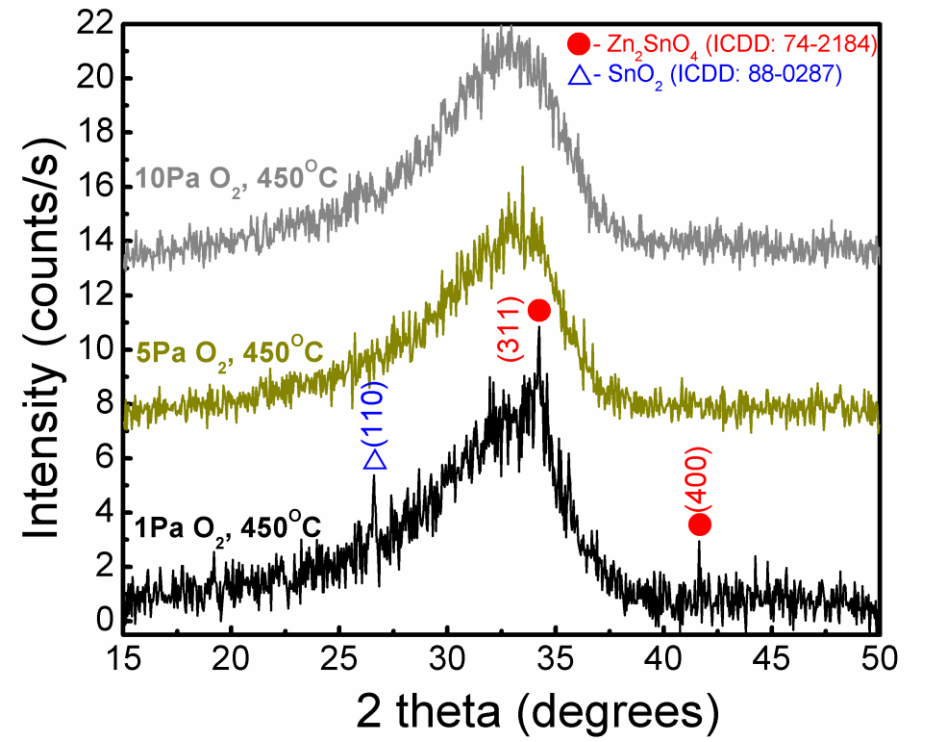

Fig. 3. XRD diffractograms of (1:1) ZnO-SnO2 samples deposited at 450 °C in 1 Pa O_2, 5 Pa O_2, 10 Pa O_2 (after annealing at 320 °C for 72h)

The transparence of ZnO-SnO_2 varied with the oxygen pressure and substrate temperature. Transmittance slightly improved after the annealing at 320 °C for 72h in air. SEM micrographs showed that the films deposited at high pressure were characterized by many cracks. All the films present droplets typical to PLD deposition. The sheet resistance of the films significantly decreases after thermal treatment. The best values were obtained for ZnO-SnO_2 samples with an atomic ratio of 1:1 and 1:3 deposited at 1 Pa oxygen pressure and 450 °C substrate temperature.

"Generation of super-thermal hadron - anti - hadron pairs using extreme light intensities", M. OANE, N. SERBAN, I. N. MIHAILESCU, JOURNAL OF INTENSE PULSED LASERS AND APPLICATIONS IN ADVANCED PHYSICS Vol. 3, No. 1, p. 7 – 10 (**2013**)

The big progress of high energy/intensity laser systems during the last years allowed for approaching new regimes of laser matter interaction. In particular, by interaction of ultra-intense laser beams with plasma, electron-positron pairs can be generated via a relativistic phenomenon, which can be described by a non-

Fourier heat equation. We conducted a brief analysis based upon Kozlowski-Kozlowska model in order to evaluate the laser parameters necessary to generate protonanti-proton pairs.

According to our analysis, the temperature in MeV (the quanta of thermal energy for electrons is about 9 eV), versus time is presented in Fig. 4.

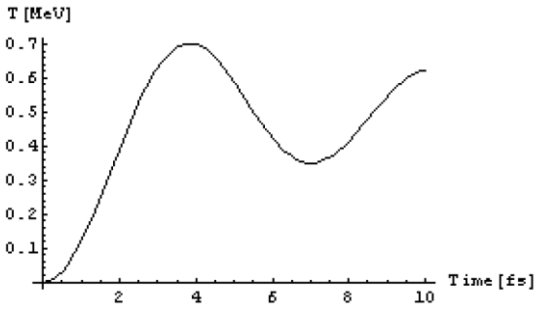

Fig. 4. Temperature versus time in the laser beam-plasma interaction

An exact analytical solution was inferred to describe the laser-solid interaction, using the Laplace transform method. We started from a previous solution describing the laser-plasma interaction and made modifications in the final formula. We expressed the temperature in MeV. As know, according to Kozlowski - Kozlowska theory, the heat can be quantified in heatons, which are express in eV. We observed that the energy was high enough to produce electron-positron pairs. We considered our results an useful tool for primary evaluations. It should be regarded as a semi-classical approach, which can be further developed, to obtain quantum heat equations.

"Influence of a hydrophobin underlayer on the structuring and antimicrobial properties of ZnO films", A. C. Popescu, G. E. Stan, L. Duta, G. Dorcioman, O. Iordache, I. Dumitrescu, I. Pasuk, I. N. Mihailescu, Journal of Materials Science 48 (23) , pp. 8329-8336 (**2013**)

Adhesion to substrate and antimicrobial efficiency of pulsed laser-deposited ZnO nanostructures were significantly increased by interposing a buffer nano-layer of hydrophobin. The hydrophobin interlayer increased by eight times the ZnO film resilience to wash in water, while in alkaline or acidic artificial sweat, it increased by 2 and 1.2 times, respectively, as compared to textiles covered with ZnO films only.

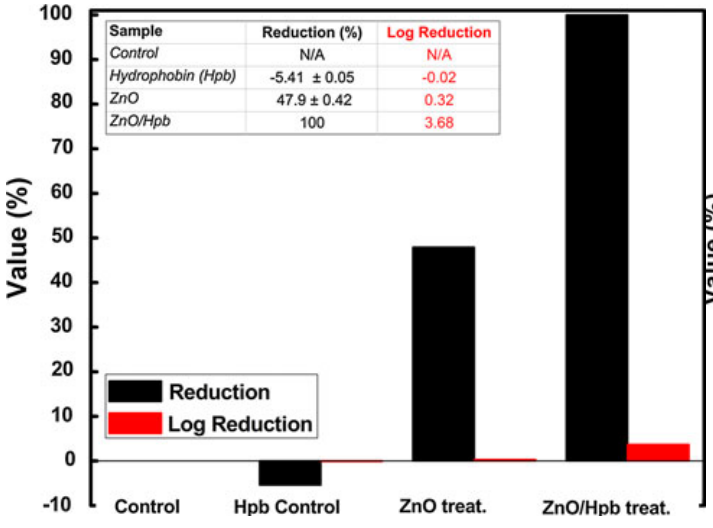

Fig. 5. Percentage and logarithmic reduction of C. albicans population

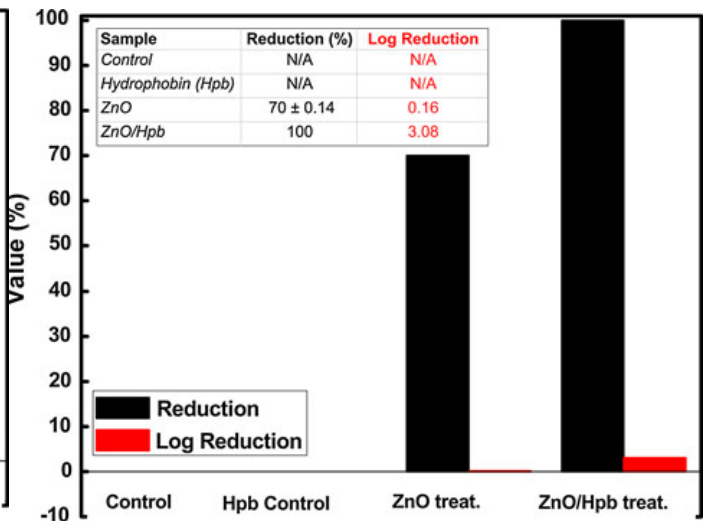

Fig. 6. Percentage and logarithmic reduction of mold mix inoculum

Hydrophobin boosted the biocide effect of ZnO nanostructured films in case of Candida albicans (Fig. 5) and mold mix inoculum (Fig. 6) cultures by 50 and 30 %, respectively. An interpretation of these phenomena is advanced based upon the results of the structural investigations. We suggest that the proposed antimicrobial finishing procedure of fabrics can find applications in the medical field, where solutions are required for eliminating microbial contaminations, thus reducing the risks of infections during surgery.

"Laser synthesis of nanometric iron oxide films for thermo-sensing applications", N. Serban, C . Ristoscu, G. Socol, N. Stefan, I. N. Mihailescu, M. Socol, S. A. Mulenko, Yu. N. Petrov, N. T. Gorbachuk, Materials Research Bulletin 1 (50), 148-154, **2014**

KrF* excimer laser pulses of 248 nm were used for the synthesis of nanometric iron oxide films with variable thickness, stoichiometry and electrical properties. Film deposition was carried out on <100> Si and SiO_2 substrates. The number of laser pulses was increased from 4,000 to 6,000, while ambient reactive oxygen pressure varied from 0.1 to 1.0 Pa. The film thickness depends on oxygen pressure, number of laser pulses and substrate nature. All films demonstrated semiconducting temperature behaviour with variable band gap (E_g) depending on oxygen pressure, substrate nature and temperature. E_g value was less than 1.0 eV for all deposited films. XRD analysis evidenced that films deposited on Si substrate have polycrystalline structure, while films deposited on SiO_2 were amorphous.

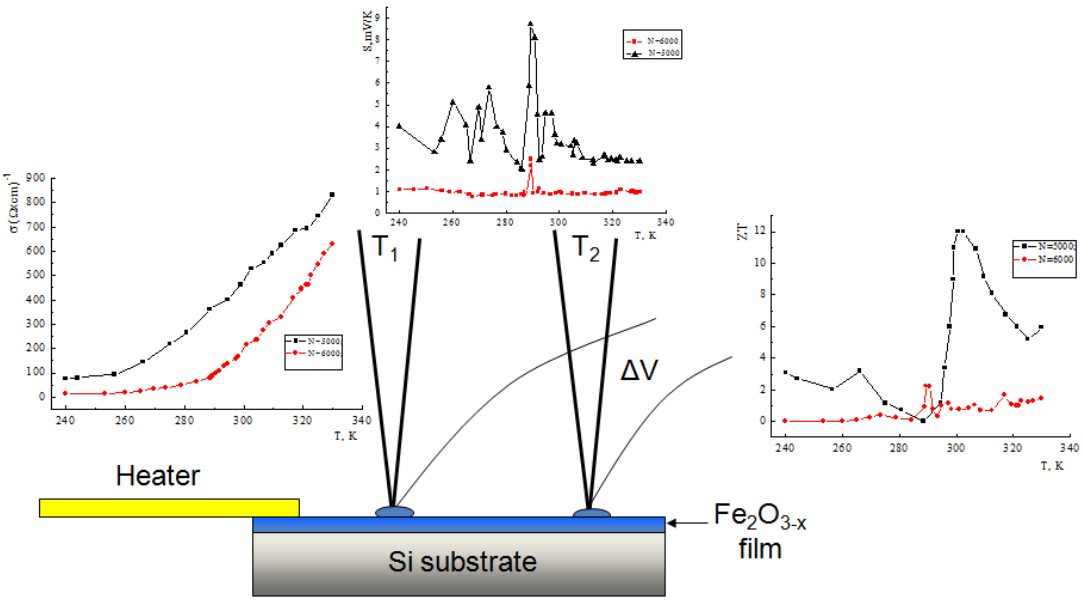

Fig. 7. Schematic representation of the electrical properties measurements set-up: temperature influence of the specific conductivity (left), S coefficient vs. temperature gradient (center) and ZT vs. temperature (right). PO_2 = 0.5 Pa, T_S = 800 K, N = 5000 or 6000.

The higher oxygen pressure, the lower crystallinity of the deposited film was observed, resulting in change of thermo electromotive force coefficient (*S*) value. For larger substrate temperature, a better crystallization was observed in the deposited films, resulting in increased *S* coefficient value. The largest value of the *S* coefficient was about 8.7 mV/K in the range 290-295 K and it decreased to 1.0-1.6 mV/K

when heating temperature changed from 240 to 330 K. The figure of merit of deposited structures was *ZT* = 3-6 in the range 240-330 K with a maximum of 12 at 300-304 K (Fig. 7). We have shown that thermo-sensing characteristics of the films strongly depend on their electrical and structural properties.

"Accurate analysis of indium-zinc oxide thin films via laser-induced breakdown spectroscopy based on plasma modeling", E. Axente, J. Hermann, G. Socol, L. Mercadier, S. A. Beldjilali, M. Cirisan, C. R. Luculescu, C. Ristoscu, I. N. Mihailescu, V. Craciun, Journal of Analytical Atomic Spectrometry 29, 553–564, **2014**

We report on accurate analysis of indium–zinc oxide thin films via laser-induced breakdown spectroscopy (LIBS) based on the calculation of the spectral radiance of the nonuniform laser-produced plasma. A thin film sample with variable elemental composition was irradiated with ultraviolet nanosecond laser pulses and the plasma emission spectra were characterized using time-resolved optical emission spectroscopy. Thus, the spectrum recorded with an Echelle Spectrometer coupled to a gated detector was compared to the spectral radiance computed for a plasma in local thermodynamic equilibrium conditions (Fig. 8). The time evolution of the plasma was studied to find optimized recording conditions for which the self-absorption of spectral lines is minimized. In addition, the time-resolved measurements allowed us to determine the Stark broadening parameters of spectral lines used for the LIBS analysis.

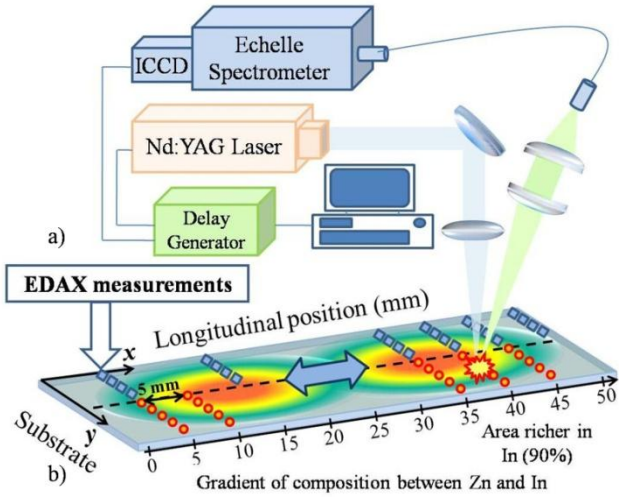

Fig. 8. LIBS setup (a). Schematic representation of a library with compositional gradient in case of IZO thin films (b). LIBS and EDS measurements were done in 11 points on the longitudinal direction of the sample

The relative atomic fraction of indium $n_{In}/(n_{In} + n_{Zn})$ deduced from the LIBS analysis is compared to the values measured by energy dispersive X-ray spectroscopy in Fig. 9 for various longitudinal positions on the sample. The EDS analyses were performed on the same sample with an estimated accuracy of a few percent. We observe a good agreement with differences smaller than 5% between the metal fractions measured by both methods. This suggests that the LIBS measurements are more accurate than the expected uncertainty of about 10% mostly due to the imprecision of spectroscopic data. The measured fraction of indium is compared to the nominal In fraction of both targets used in the combinatorial pulsed laser deposition process (dashed blue lines in Fig. 9). The measured maximum and minimum values slightly differ from the nominal In fractions in the targets. This is attributed to the expansion dynamics of the ablation plume that produces compositional intermixing on the substrate during the deposition process. The observed good agreement between LIBS and EDS measurements indicates that the precision of the used Einstein coefficients of spontaneous emission is probably better than 10%.

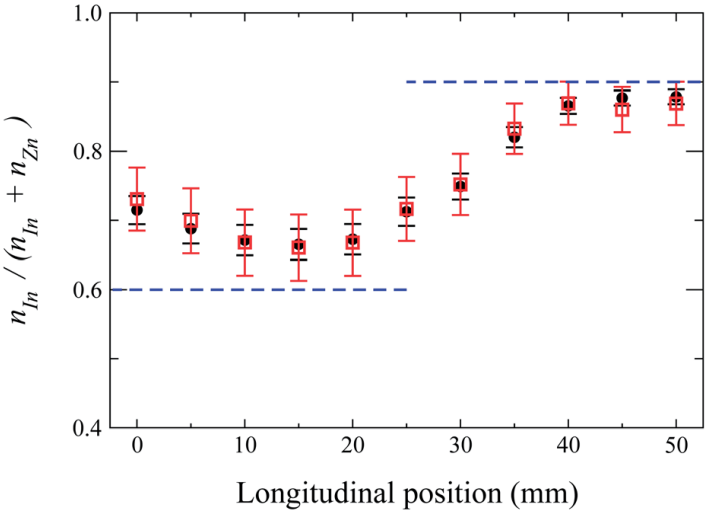

Fig. 9. Atomic fraction of indium compared to the total metal content within the thin film versus the longitudinal position on the sample. The fractions measured by LIBS and EDS are represented by empty red and filled black symbols, respectively. The dashed lines represent the indium fractions of the targets used for thin film synthesis by Combinatorial-PLD.

The present results show that LIBS measurement procedures based on plasma modeling could be used for fast quality control in the industrial production of thin films.

"Ultra high molecular weight polyethylene acetabular cups functionalized with bioactive glass coatings synthesized by pulsed laser deposition", L. Duta, A. C. Popa, F. Miculescu, I. N. Mihailescu, Romanian Reports in Physics, Vol. 66, No.3, P. 788–800, **2014**

We have synthesized bioactive glass (BG) coatings onto commercial ultra high molecular weight polyethylene (UHMWPE) acetabular cup implants by Pulsed Laser Deposition using a SiO_2–Na_2O–K_2O–CaO–MgO–P_2O_5 BG compositional system, and tested them for 42 days by immersion in simulated body fluid, in homeostatic conditions. Structural (FTIR), morphological (SEM) and compositional (EDS) measurements assessed the PLD method feasibility for producing high quality implant coatings. The FTIR measurements showed highly depolymerized network for the BG which was able to induce the nucleation, growth and structuring of a biologically active apatite layer *in vitro*, with chemical composition resembling the one of human bone. The SEM investigations showed the conversion of the typical PLD film surface (consisting of round-shaped micrometric particulates) into a rough homogenous surface with an acicular aspect. The EDS analysis showed a remarkable nearly-stoichiometric transfer of the target composition to the BG deposited films.

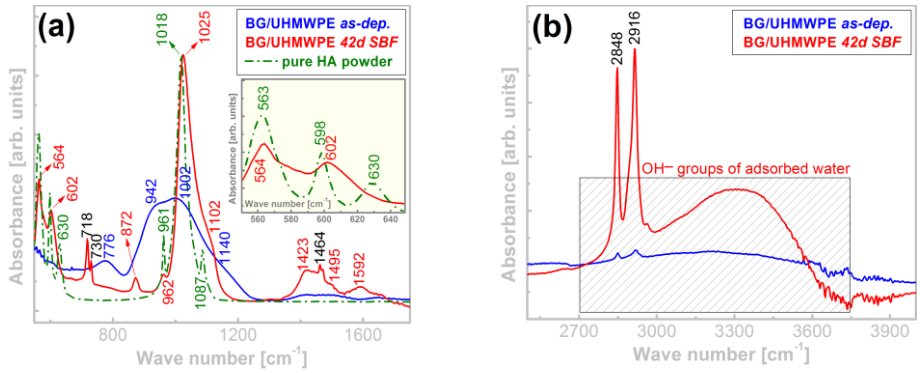

Fig. 10. Detailed FTIR spectra of BG61 coatings prior (blue line) and after (red line) the immersion in SBF for 42 days: a) 1750–550; b) 4000–2500 cm^{-1} range zoom.

In Fig. 10 one can observe the detailed FTIR spectra of BG61 samples for two different wave number domains: (1750–550) and (4000–2500) cm-1, respectively. The lower intensity spectrum (blue line) belongs

to the as-deposited BG61 coating, whilst the one with sharper peaks (red line) was recorded in case of the implant coating after 42 days of immersion in SBF.

Our findings demonstrate a high *in vitro* biomineralization capacity of the BG coating, favorable for a rapid osteointegration of implants. We conclude that BG/UHMWPE structures show promise for use as highly bioactive materials for applications in regenerative medicine.

"Antifungal activity of Ag:hydroxyapatite thin films synthesized by pulsed laser deposition on Ti and Ti modified by TiO_2 nanotubes substrates", S. Eraković, A. Janković, C. Ristoscu, L. Duta, N. Serban, A. Visan, I.N. Mihailescu, G.E. Stan, M. Socol, O. Iordache, I. Dumitrescu, C.R. Luculescu, Dj. Janaćković, V. Miškovic-Stanković, Applied Surface Science, 293, 37-45, **2014**

We have applied PLD to assemble HA and Ag:HA thin films on the surface of pure Ti and Ti modified by TiO2 nanotubes substrates. A quasi-stoichiometric target-to-substrate transfer was ascertained by EDS, whilst the restoration of the crystalline status after post-deposition heat-treatment performed at 500 ◦C in water vapors for 6 h was confirmed by the FTIR and XRD analyses. Thus, benefic effects on the long term stability of these films in biological fluids should be expected. We have shown by AFM that Ag:HA thin films exhibit nanostructured topography which is prone to allow a better biointegration of the implant.

Dedicated cytotoxicity tests of glass control, Ti substrate, $nTiO_2$/Ti substrate, and Ag:HA/$nTiO_2$/Ti coating have been conducted. The results were at the basis of our choice for conducting the microbiological antifungal testing on the crystalline Ag:HA thin films deposited on Ti modified by TiO_2 nanotubes substrates. The tests were conducted against two common pathogenic fungal strains, *C. albicans* and *A. niger* (Fig. 11). The biological assays demonstrated the high antifungal efficiency of heat-treated Ag:HA thin films deposited on Ti modified by TiO_2 nanotubes substrates which completely exterminate *C. albicans* and radically reduce the *A. niger* number of colonies.

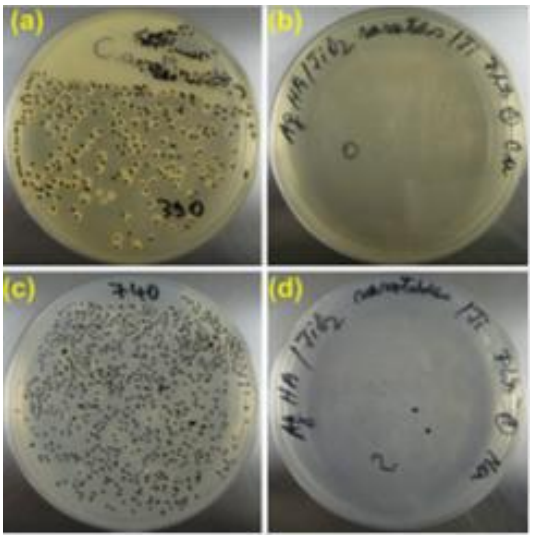

Fig. 11. Comparative photographs of fungal populations (Candida albicans – a and b; Aspergilus niger – c and d), 24 h after incubation, on the heat-treated Ag:HA/$nTiO_2$/Ti films (b and d) and standard control samples (a and c).

Our conclusion is that the deposition by PLD of Ag:HA thin films on Ti modified with TiO_2 nanotubes substrates followed by a heat treatment at 500 ◦C in water vapors for 6 h, allows for the fabrication of efficient shield barriers against adherence and contamination by pathogenic fungi.

"Biomimetic nanocrystalline apatite coatings synthesized by Matrix Assisted Pulsed Laser Evaporation for medical applications", A. Visan, D. Grossin, N. Stefan, L. Duta, F.M. Miroiu, G.E. Stan, M. Sopronyi, C. Luculescu, M. Freche, O. Marsan, C. Charvilat, S. Ciuca, I.N. Mihailescu, Materials Science and Engineering B 181, 56-63, **2014**

We performed the deposition of adherent biomimetic nanocrys-talline apatite thin films by matrix-assisted pulsed laser evaporation (MAPLE) technique onto titanium and silicon substrates. The FTIR and Raman spectra of the thin films were found to be highly similar and had an identical signature to the spectrum of the initial powder. The observed shoulders attributed to theHPO_4^{2-} non-apatitic ions confirm the preservation of a hydrated phase inside the thin films. A very limited transformation of the initial nanocrystals was observed, whilst the original chemical composition of the starting powders was preserved. The BmAp biomaterials in the form of thin films showed a high resemblance to the human hard tissue mineral structure and composition, and are therefore expected to insure a better functionality to metallic implant coatings (Fig. 12).

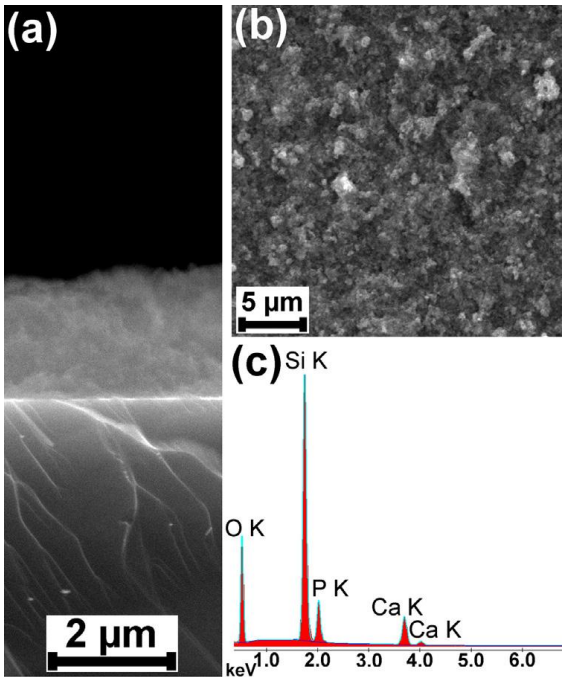

Fig. 12. SEM micrographs recorded in cross-view (a) and top-view modes (b) for theBmAp MAPLE film. EDS spectrum for the BmAp MAPLE film (c)

We conclude that the MAPLE method is capable to maintain the structural fidelity after transfer of biomimetic apatite from a solid frozen target to a nearby substrate, in form of thin film. We have thus obtained and put in evidence the complete transfer of a hydrated, delicate material by MAPLE. To the best of our knowledge, this is the first report of MAPLE deposition of thin films of poor-crystallized hydrated apatites synthesized by the biomimetic method.

"Pulsed laser deposition synthesis of non-metal doped TiO_2/ZrO_2 thin films: electronic structure and optical and photocatalytic characteristics", O.Linnik, N. Shestopal, N. Smirnova, A. Eremenko, O. Korduban, V. Kandyba, T. Kryshchuk, G. Socol, N. Stefan, G. Popescu-Pelin, C. Ristoscu, I. N. Mihailescu, Vacuum (**2015**) 10.1016/j.vacuum.2014.12.011

TiO_2/ZrO_2 thin films doped with N, C and/or O were synthetized by pulsed laser deposition in low-pressure, chemically active gaseous mixtures. Photocatalytical activity of the obtained structures was studied against reduction of toxic bichromate ions. A direct correlation was observed between the presence of ZrO_2, the

type and level of doping with N, C and/or O, the absorption in UV and visible range and the efficiency of the reduction reaction. The best conversion was achieved in case of ZrO_2(10%)/TiO_2 films deposited in N_2/CH_4 (5:1) mixture at a total pressure of 1 mbar. The correlation between the zirconia content and the efficiency of substitutional N incorporation was noticed. It was supposed that the distortion of $Ti^{4+}O_2$ lattice with the advent of Ti^{3+} states occurred due to the larger radius of zirconium ions (R_{Zr4+}=0.720Å as compared to R_{Ti4+}= 0.650 Å). The relative high stability of Ti^{3+} states was assigned to the presence of Zr^{4+} ions. The highest conversion percent of photoreduced Cr(VI) ions under UV (51%) and visible irradiation (14%) was reached in the case of ZrO_2(10%)/TiO_2 obtained in N_2/CH_4 (5:1) atmosphere and 1 mbar pressure.The possible contribution of both substitution of O to N and concomitant oxygen vacancies in the oxide matrix to additional visible-light absorption should also be considered. It is suggested that the level of the interstitial N atoms in TiO_2 matrix (rather than TiO_{2-x}) is essential for photocatalytic reduction of bichromate ions under both UV and visible light (Fig. 13)

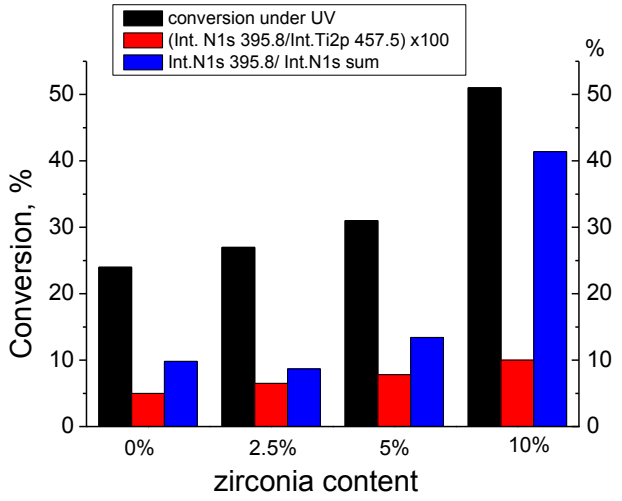

*Fig. 13. Influence of zirconia content in **ZrTiN5C1** films on the photocatalytic conversion under UV (black column), ratio of N1s at 395.8 eV to Ti2p at 457.5 eV (red column) and N1s at 395.8 eV to total N1s (blue column)*

"Structural and biological evaluation of lignin addition to simple and silver doped hydroxyapatite thin films synthesized by matrix-assisted pulsed laser evaporation", A. Janković, S. Eraković, C. Ristoscu, N. Mihailescu (Serban), L. Duta, A. Visan, G.E. Stan, A.C. Popa, M.A. Husanu, C.R. Luculescu, V.V. Srdić, Dj. Janaćković, V. Mišković-Stanković, C. Bleotu, M.C. Chifiriuc, I.N. Mihailescu, Journal of Materials Science: Materials in Medicine, 26 (**2015**) 17

We report on thin film deposition by MAPLE of simple hydroxyapatite (HA) or silver (Ag) doped HA combined with the natural biopolymer organosolv lignin (Lig) (Ag:HA-Lig). Solid cryogenic target of aqueous dispersions of Ag:HA-Lig composite and its counterpart without silver (HA-Lig) were prepared for evaporation using a KrF* excimer laser source. The expulsed material was assembled onto TiO_2/Ti substrata or silicon wafers and subjected to physical and chemical investigations.

Smooth, uniform films adherent to substratum were observed. The chemical analyses confirmed the presence of the HA components, but also evidenced traces of Ag and Lig. Deposited HA was Ca deficient, which is indicative of a film with increased solubility. Recorded X-ray Diffraction patterns were characteristic for amorphous films. Lig presence in thin films was undoubtedly proved by both X-ray Photoelectron and Fourier Transform Infra-Red Spectroscopy analyses. The microbiological evaluation

showed that the newly assembled surfaces exhibited an inhibitory activity both on the initial steps of biofilm forming and on mature biofilm development formed by bacterial and fungal strains. The intensity of the anti-biofilm activity was positively influenced by the presence of the Lig and/or Ag, in the case of *Staphylococcus aureus*, *Pseudomonas aeruginosa* and *Candida famata* biofilms. The obtained surfaces exhibited a low cytotoxicity toward human mesenchymal stem cells (Fig. 14), being therefore promising candidates for fabricating implantable biomaterials with increased biocompatibility and resistance to microbial colonization and further biofilm development.

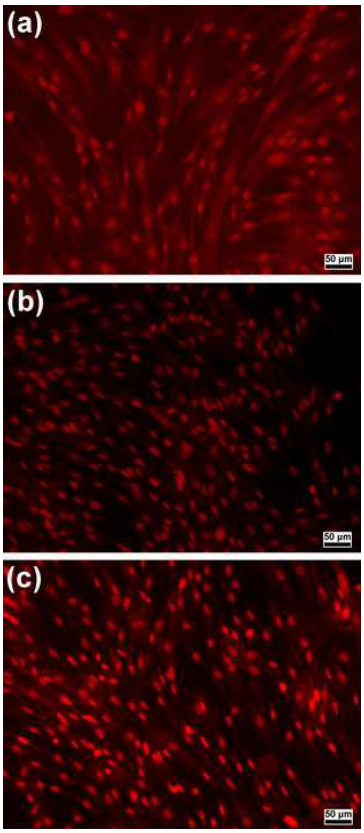

Fig. 14. Fluorescence microscopy images of nuclei of WJ-MSCs grown on different substrata: pure HA (a); HA-Lig (b); and Ag:HA-Lig (c) films. Magnification: 200X

In conclusion, the microbiological assays showed that the coated composite secured a prolonged release of silver ions, being protective both against the initial phase of microbial colonization and the mature biofilm development. The lignin addition boosted the anti-microbial activity of HA doped with silver ions against both bacterial and fungal biofilms. An implant surface modified in such a manner could host osteogenic cell proliferation while shielding from bacteria and fungi, thus facilitating a safe osteointegration of the medical device.

"Temperature control of crystalline status and phenomenological modes", T. Rosca, S. Bazgan, G. Dorcioman, C. Ristoscu, G. Popescu-Pelin, N. Enaki, I. N. Mihailescu, Romanian Reports in Physics 3 (**2016**)

A phenomenological model describing the nonlinear process of the growth of *Ti* and TiO_2 films on *Si* or SiO_2 substrates is proposed. It is considered that bound electrons from the *Si* surface are coupled with energy inferior to that of the electrons in the bulk of the *Si* substrate. The transition from crystalline to vitreous phase in the deposited films is analyzed based upon the nonlinear theory of phase transitions.

It is supposed that the electrons on the *Si* surface are coupled due to existence of voids in the crystalline continuity and have a smaller coupling energy than the electrons forming covalent bonds between *Si* atoms of the crystalline substrate (Fig. 15). Correspondingly, the coupled energy can be easily dropped by the *Ti* atoms relaxing on surface. When the TiO_2 radicals get closer to surface, the unpaired electrons can break the weak coupled pairs of electrons from the surface bounds so that *Si* crystalline lattice is growing with *Ti* material. This is possible due to the fact that the coupled electrons to the substrate surface of *Si* reach a more stable state when entering into a new electronic bond (covalent or ionic) with TiO_2. Thus, the surface starts are arranged as a new crystal lattice of TiO_2.

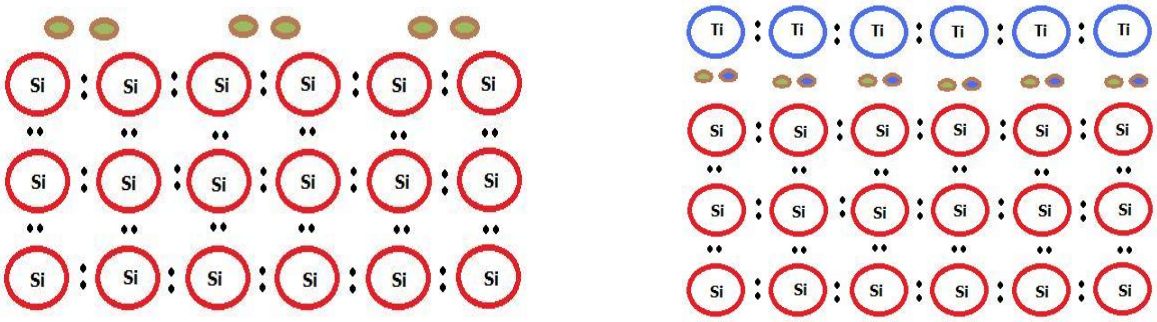

Fig. 15. Chemical bounding in Si and Si-Ti systems. Electronic couples of Si substrate are represented by dark points. The electrons at the interface forming weak coupling are represented by green dots. The Ti atoms close to surface break those ties creating a continuously growing network crystalline

We defined the non-harmonic potential function for the vibration of each *Ti* atom around the equilibrium position. Starting with a specific value of phenomenological parameters of this potential, the system passes from crystalline to glass growth. These parameters are connected to the temperature and thermodynamic functions characteristic to involved materials. The connection of these parameters to the entropy, heat capacity, critical temperature and sound velocity were studied. Our approach permits to construct the phenomenological potential in the glass deposition which can be applied to the estimation of the mean size of the disorders in the glass forming in the growing material. The theory allows for the construction of the potential function $V(u)$ which when increasing the temperature becomes double holes potential. This second hole becomes random for each *Ti* atom of growing materials. However, under this situation, it is possible to statistically average the double hole potential and find the new connection between the theoretical model and the experimental data.

Spying on Qubit G400 gas mixing system

The purpose of this work was to extend the functional possibilities of the G400 system, by attaching time stamps to Open or Close commands sent to valves and producing log files that contain both the commands sent to gas controllers and reports received from them about the status of the system. This necessity appeared as the control software provided by the manufacturer of the G400 system doesn't produce a log file and has no means to interact with other software or hardware.

The timing information thus obtained can be used to control or supervise other equipment in the experimental setup involving the G400 system and give the possibility to correlate the change of various parameters of interest with the moments when the gas mix begins to flow into the experimental setup (or when it stops to be fed up).

The documentation provided with the system and associated software being scarce with details about the internal system workings, the most difficult part of presented work included a large amount of reverse engineering performed to obtain the needed information.

In the configuration used at INFLPR the G400 system has 4 gas controllers holding the logo Qbit Systems and one controller AALBORG model DFC26 (Fig. 16).

Fig. 16: Qubit G400 gas mixing system in LSPI laboratory, INFLPR

Other publications with acknowledgements to this contract, which were not presented in this report:

1. „Generation of super-thermal hadron - anti - hadron pairs using extreme light intensities", M. Oane, N. Serban, I. N. Mihailescu, Journal of Intense Pulsed Lasers and Applications in Advanced Physics vol. 3, no. 1, p. 7 – 10, **2013**

2. „Semi-analytical model of two-photon thermal effects in laser scanning of solids", Mihai Oane, Natalia Serban, Dorina Toader, Ion N. Mihăilescu, Journal of Intense Pulsed Lasers and Applications in Advanced Physics 3(3), 37-40, **2013**.

3. "Biological hydroxyapatite thin films synthesized by pulsed laser deposition", L.Duta, N. Serban, F.N. Oktar, I.N. Mihailescu, OPTOELECTRONICS AND ADVANCED MATERIALS – RAPID COMMUNICATIONS Vol. 7, No. 11-12, p. 1040-1044, **2013**

4. „Multiple nano-second laser ablation of metals based upon a new two-temperature approach", N. Serban, M. Oane, I. N. Mihailescu, Romanian Reports in Physics, Vol. 65, No. 3, P. 979–983, **2013**

5. „Visible light-harvesting of TiO_2 nanotubes array by pulsed laser deposited CdS", Bjelajac, Andjelika; Djokic, Veljko; Petrovic, Rada; Socol, Gabriel; Mihailescu, Ion N.; Florea, Ileana; Ersen, Ovidiu; Janackovic, Djordje; APPLIED SURFACE SCIENCE Volume: 309 Pages: 225-230 Published: AUG 1 **2014**

6. "A new concept of stainless steel medical implant based upon composite nanostructures coating",L. Floroian, M. Florescu, D. Munteanu, M. Badea, G. Popescu-Pelin, C. Ristoscu, F. Sima, M.C. Chifiriuc, I.N. Mihailescu, Digest Journal of Nanomaterials and Biostructures, 9 (4), October – December **2014**, 1555-1568

7. *"Phenomenological model of growth of TiO_2 films for biomedicine",* S Bazgan, I. Cojocaru, T. Rosca, G Dorcioman, C. Ristoscu, G. Popescu-Pelin, N. Enaki, I.N. Mihailescu, Paper 9258 – 43 in SPIE Proceedings of Advanced Topics in Optoelectronics, Microelectronics, and Nanotechnologies **2014** (OMN14), Constanta, Romania, August 21 - 24, 2014

Project Manager,

Prof. Dr. Ion N. Mihailescu